

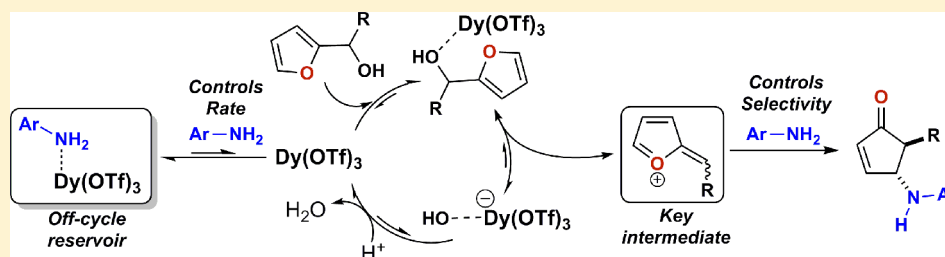
Importance of Off-Cycle Species in the Acid-Catalyzed Aza-Piancatelli Rearrangement

Diana Yu,[†] Van T. Thai,[†] Leoni I. Palmer,[‡] Gesine K. Veits,[‡] Jonathan E. Cook,[‡] Javier Read de Alaniz,[‡] and Jason E. Hein^{*†}

[†]Chemistry and Chemical Biology, University of California, Merced, California 95343, United States

[‡]Department of Chemistry and Biochemistry, University of California, Santa Barbara, California 93106, United States

S Supporting Information



ABSTRACT: The observed rate of reaction in the dysprosium triflate catalyzed aza-Piancatelli rearrangement is controlled by a key off-cycle binding between aniline and catalyst. Deconvoluting the role of these ancillary species greatly broadens our understanding of factors affecting the productive catalytic pathway. We demonstrate that the rate of reaction is controlled by initial competitive binding between the furylcarbinol and nitrogen nucleophile using either a Brønsted or Lewis acid catalyst and that the resulting rearrangement proceeds without involving the Brønsted and Lewis acid catalyst. This shows conclusively that the rate-controlling step and selectivity of reaction are decoupled.

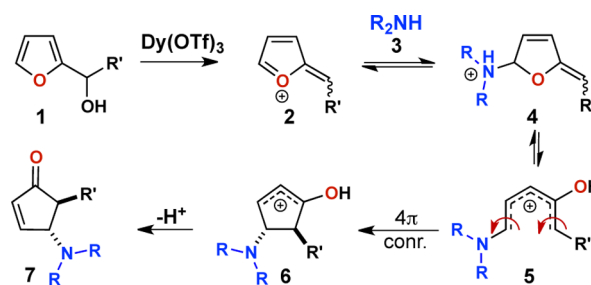
The Piancatelli rearrangement, first reported in 1976, is a powerful method for accessing valuable substituted cyclopentenones and has been extensively employed for the synthesis of prostaglandin derivatives.¹ While the Piancatelli rearrangement has been primarily used to construct 4-hydroxycyclopentenones, it also holds tremendous promise for directly accessing other valuable building blocks. Recently, processes have emerged that allow anilines,² alcohols,³ and electron-rich aromatic amides⁴ to participate in the cascade rearrangement. Despite the steady progress in this area, the development of a catalyst system that can improve reactivity and expand the range of nucleophiles has been hampered by a lack of mechanistic understanding.

During our development of a dysprosium triflate ($\text{Dy}(\text{OTf})_3$) catalyst system that allows anilines to participate in the Piancatelli rearrangement, we made several observations that prompted us to further investigate this molecular rearrangement from a kinetic and mechanistic point of view. We sought to provide mechanistic evidence to aid in the design of improved catalysts and reaction protocols. Specifically we were interested in addressing three major questions: First, what is the role of the catalyst in the reaction? Second, what are the origins of the previously noted electronic effects of the aniline nucleophile on reaction rate?^{2b} Third, why is the cascade rearrangement of furylcarbinols restricted to aniline nucleophiles?

The aza-Piancatelli rearrangement is thought to be initiated by the formation of an oxocarbenium intermediate **2**, via the

action of an appropriate Brønsted or Lewis acid catalyst (Scheme 1). Attack of aniline **3** at the 5' position of the furan

Scheme 1. Proposed Intermediates in the Aza-Piancatelli Rearrangement



generates amination **4**. Ring-opening gives pentadienyl cation **5**, which then undergoes 4π conrotatory electrocyclic closure to give the *trans*-substituted cyclopentenone **7** through the corresponding oxallyl cation **6**. While theoretical calculations by de Lera provided support for the stereoselective C–C bond-forming 4π -conrotatory cyclization process in the Piancatelli rearrangement,⁵ a kinetic and mechanistic view of the sequence of events prior to the electrocyclic closure was unknown. In this work, we

Received: October 2, 2013

Published: December 4, 2013

report detailed kinetic studies of the aza-Piancatelli rearrangement catalyzed by both Brønsted and Lewis acid catalysts.

Our initial investigations centered on probing the role of different catalysts, Brønsted or Lewis acid, on the reaction. It is known that rare earth metal triflates ($\text{RE}(\text{OTf})_3$) can release trace amounts of triflic acid, which could be responsible for catalysis.⁶ In our original report, potassium carbonate shut down Brønsted, but not Lewis acid catalysis, suggesting that catalysis indeed involved $\text{Dy}(\text{OTf})_3$ directly.^{2a} To further investigate the role of the catalyst, furfurylcarbinol **8** and aniline **9a** were subjected to reaction conditions utilizing trifluoroacetic acid (TFA) or $\text{Dy}(\text{OTf})_3$ as the catalyst. TFA was chosen instead of triflic acid because it gave cleaner conversion to cyclopentenone **7**.⁷ The reaction progress was monitored via continuous in situ analysis using ReactIR (Figure 1). Changes

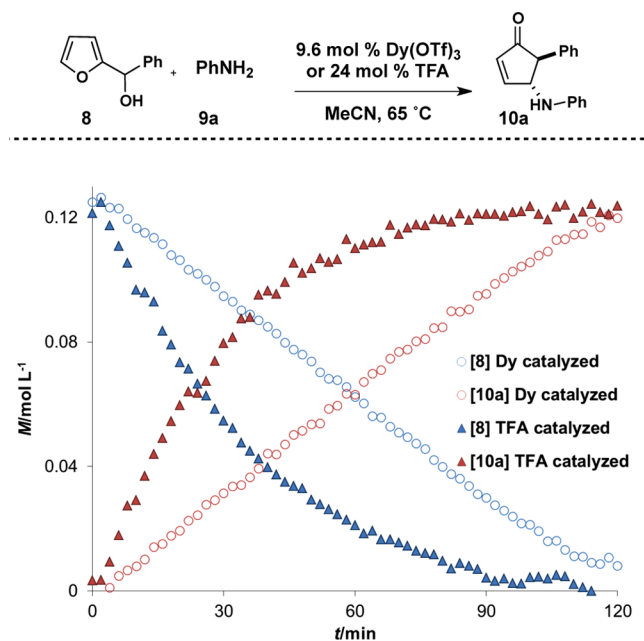


Figure 1. Reaction progress for Brønsted or Lewis acid catalyzed processes.

in reagent and product concentration were validated independently using HPLC/MS via sampling throughout the reaction. Surprisingly, we found that the TFA-catalyzed reaction was first order in substrate and first order in TFA ($[\text{TFA}] = 3.3\text{--}30.0\text{ mM}$), while the $\text{Dy}(\text{OTf})_3$ -catalyzed reaction is zero-order in substrate and first-order in $\text{Dy}(\text{OTf})_3$ ($[\text{Dy}(\text{OTf})_3] = 2.0\text{--}12.0\text{ mM}$).⁸

The variation in the observed order confirms that the reaction is indeed catalyzed by $\text{Dy}(\text{OTf})_3$ and is not being promoted by adventitious generation of triflic acid under the reaction conditions. In addition, this result implies that the resting state of the catalyst is different when a Brønsted or Lewis acid is utilized.

To test the role of the nucleophile in the reaction, a further investigation into the effect of the electronic nature of the aniline was next initiated. We previously noted marked effects qualitatively on rates in both the inter- and intramolecular aza-Piancatelli rearrangement depending on the aniline employed.² Indeed, when the reaction was monitored in situ, the electronic character of the aniline nucleophile was found to have a dramatic impact on the reaction rate when either a Lewis or Brønsted acid catalyst was employed. This was illustrated via a

linear free energy correlation for a series of *para*-substituted anilines (Figure 2), giving a Hammett ρ value for the $\text{Dy}(\text{OTf})_3$

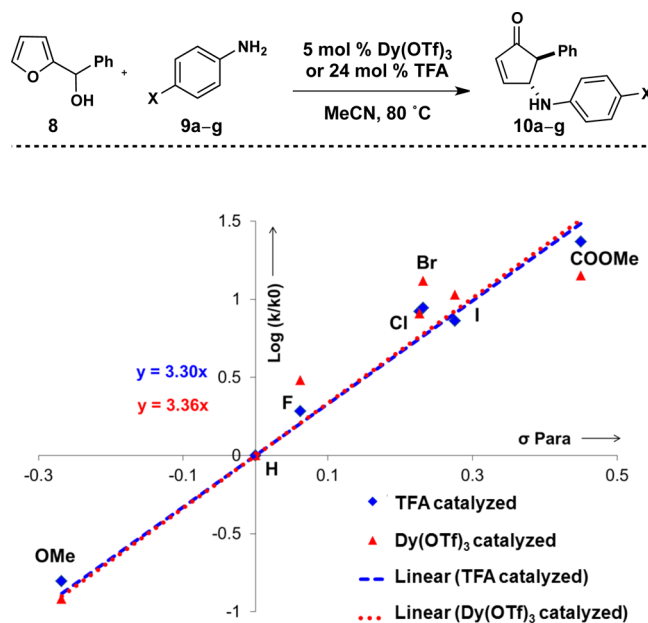


Figure 2. Linear free energy relationship using *para*-substituted anilines under either Brønsted or Lewis acid catalysis.

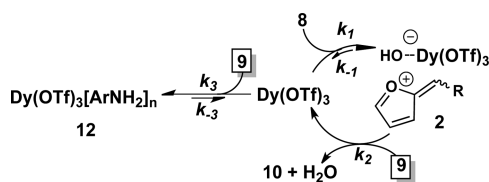
and TFA-catalyzed reactions of +3.36 and +3.30, respectively. This remarkable agreement implies that the relative change in rate is due to a common phenomenon, regardless of the observed first-order (TFA) or zero-order ($\text{Dy}(\text{OTf})_3$) behavior.

The combined observations of a zero-order reaction profile and large positive values for ρ in the $\text{Dy}(\text{OTf})_3$ -catalyzed aza-Piancatelli rearrangement can be rationalized in one of two ways. First, ring-opening of the aminal **4** may be the rate-limiting step in the catalytic cycle. The analogous spirocyclic acetal species have been isolated in the oxa-Piancatelli reaction and were found to be stable and catalytically competent.^{3,9} However, aminal **4** has never been observed in the aza-Piancatelli rearrangement. Moreover, electron-donating groups would be expected to stabilize the proposed cationic intermediates, resulting in a negative ρ value.

Alternatively, reversible preferential binding of the dysprosium catalyst by the aniline nucleophile may be responsible for both the positive ρ value and zero-order reaction profile. While the lanthanides are generally regarded as strongly oxo-philic species, tight coordination to the more Lewis basic nitrogen species could form an inactive, coordinatively saturated complex **12** (Scheme 2).

This model is similar to competitive inhibition in Michaelis–Menten kinetics;¹⁰ however, aniline **9** serves both as the nucleophile capturing oxocarbenium **2** in the productive cycle and as the inhibitor, sequestering free catalyst as complex **12**. If

Scheme 2. Competitive Binding of $\text{Dy}(\text{OTf})_3$



we assume strong binding between aniline **9** and free catalyst ($k_3 \gg k_1$ and k_{-3}) and that addition to oxocarbenium **2** is fast ($k_2 \gg k_1$ and k_{-1}) the steady-state rate equation can be expressed as eq 1.

$$\frac{d[10]}{dt} = \frac{k_1 k_{-3} [8][\text{Dy}(\text{OTf})_3]}{k_3 [9]} \quad (1)$$

This expression demonstrates the push–pull effect that both substrates can have, resulting in the rate of reaction being proportional to the ratio of furylcarbinol **8** to aniline **9**. In addition, this expression also illustrates the magnitude that the off-cycle dissociation constant, given by k_{-3}/k_3 , has on the observed rate. Thus, the drop in reaction rate with electron-rich anilines can be attributed to a tighter binding between aniline and $\text{Dy}(\text{OTf})_3$ leading to a shift in the equilibrium toward **12**.

To investigate the off-cycle binding of $\text{Dy}(\text{OTf})_3$ by aniline further, we carried out a series of experiments where the ratio of aniline to furylcarbinol was varied. Reactions with excess of furylcarbinol **8** showed an initial rate of 1.1 mM/min, while systems with excess aniline **9a** display a slower 0.26 mM/min. However, the reactions could be modified by adding sufficient aniline **9a** (Figure 3A) or furylcarbinol **8** (Figure 3B) to give equimolar reaction mixtures, now displaying similar rates (6.5 and 5.1 mM/min, respectively).

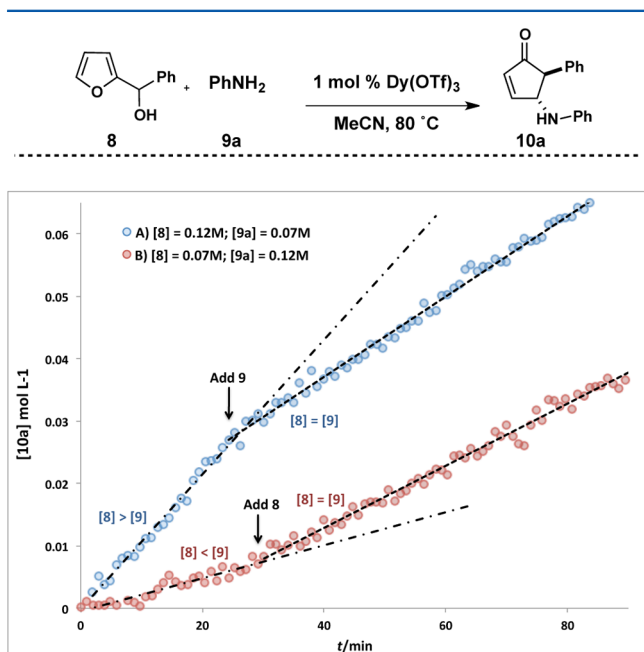


Figure 3. Effect of excess aniline or furylcarbinol on $\text{Dy}(\text{OTf})_3$ -catalyzed cycloaddition.

These results indicate that the major factor contributing to the observed rate of reaction is off-cycle binding of the dysprosium catalyst as a complex such as **12** (Scheme 2) and, further, that the binding equilibrium between free dysprosium, aniline binding, or furylcarbinol binding lies very far in favor of amine complex **12**. While we were not able to isolate an authentic species such as **12**, several stable aniline-dysprosium species have been reported and characterized.¹² In addition, the observed zero-order reaction profile for this rearrangement is similar to a proline-catalyzed system where off-cycle catalyst binding restricts the available catalyst pool.¹³

These data suggest that performing the reaction in the presence of a limited quantity of aniline would be beneficial to achieve a higher rate of reaction. However, HPLC analysis of experiments with excess aniline consistently gave higher yields of cyclopentenone **10a**. This is due to the formation of byproducts via competitive Friedel–Crafts alkylation and decomposition of the oxocarbenium intermediate **2**, which is exacerbated when the aniline nucleophile is limited.¹⁴

The selectivity of the cycloaddition was examined in the presence of multiple aniline nucleophiles (Figure 4). The reaction was performed using furylcarbinol **8** (0.125 M) with *p*-Cl and *p*-OMe aniline (**9b** and **9c**, respectively, 0.0625 M each) and either $\text{Dy}(\text{OTf})_3$ or TFA. Aliquots were withdrawn at regular time points and analyzed by HPLC/MS to give the rate of formation of both **10b** and **10c**, revealing that, initially, cyclopentenone **10c** is formed faster than **10b**, regardless of the mode of catalysis (Figure 4a and b).

Given that individually the cycloaddition with *p*-Cl aniline **9b** is much faster than with *p*-OMe aniline **9c** (Figure 2) the competition result appears initially surprising. However, these observations are consistent with a mechanism where reversible off-cycle binding between aniline and catalyst (either H^+ or $\text{Dy}(\text{OTf})_3$) is responsible for the difference in rate in the competition reaction (Scheme 3, K_1 vs K_2). This feature is evident from the rate of formation of **10b**, which increases near the end of the reaction (Figure 4a, ~90 min), corresponding to the point at which *p*-OMe aniline **9c** is exhausted. Thus, complex **15** is initially formed with the more electron-rich **9c**; however, once the *p*-OMe aniline is expended, complex **16** persists. The difference in rate between the initial and later portion of the reaction would be due to a difference in the equilibrium constant for free $\text{Dy}(\text{OTf})_3$ and complex **15** and **16**. An analogous case exists for the TFA-catalyzed system, where the relative basicity of the substituted aniline modulates the concentration of acid available to conduct catalysis.

The selectivity in the competition reaction results from a difference in nucleophilicity between *p*-OMe and *p*-Cl aniline (k_1 vs k_2), clearly demonstrating that the rate of product formation is decoupled from the selectivity-determining step in the reaction. This result indicates that the role of either Lewis or Brønsted acid catalyst is limited to the formation of the key oxocarbenium intermediate **2** and is not directly involved in the subsequent electrocycloaddition event.

In summary, we have demonstrated that the aza-Piancatelli rearrangement displays a unique reaction profile depending on whether a Lewis ($\text{Dy}(\text{OTf})_3$) or Brønsted (TFA) acid is employed. The initial competitive binding between $\text{Dy}(\text{OTf})_3$ or TFA and the aniline restricts the concentration of available catalyst for the formation of the oxocarbenium ion that triggers the rearrangement. This key equilibrium rationalizes the dependence of reaction rate on differently substituted anilines. In addition, this trend explains why weakly nucleophilic compounds (such as anilines) are compatible substrates, while more basic amines (such as morpholine) do not participate in the reaction. Finally, the competition experiments indicate that the selectivity of the reaction is determined by the relative nucleophilicity of the two anilines, not on the observed rate of reaction for the independent substrates.

EXPERIMENTAL SECTION

General Remarks. Furan-2-yl(phenyl)methanol was prepared according to literature precedent of a similar transformation by reacting furfural with phenylmagnesium bromide.¹⁵ Dysprosium(III)

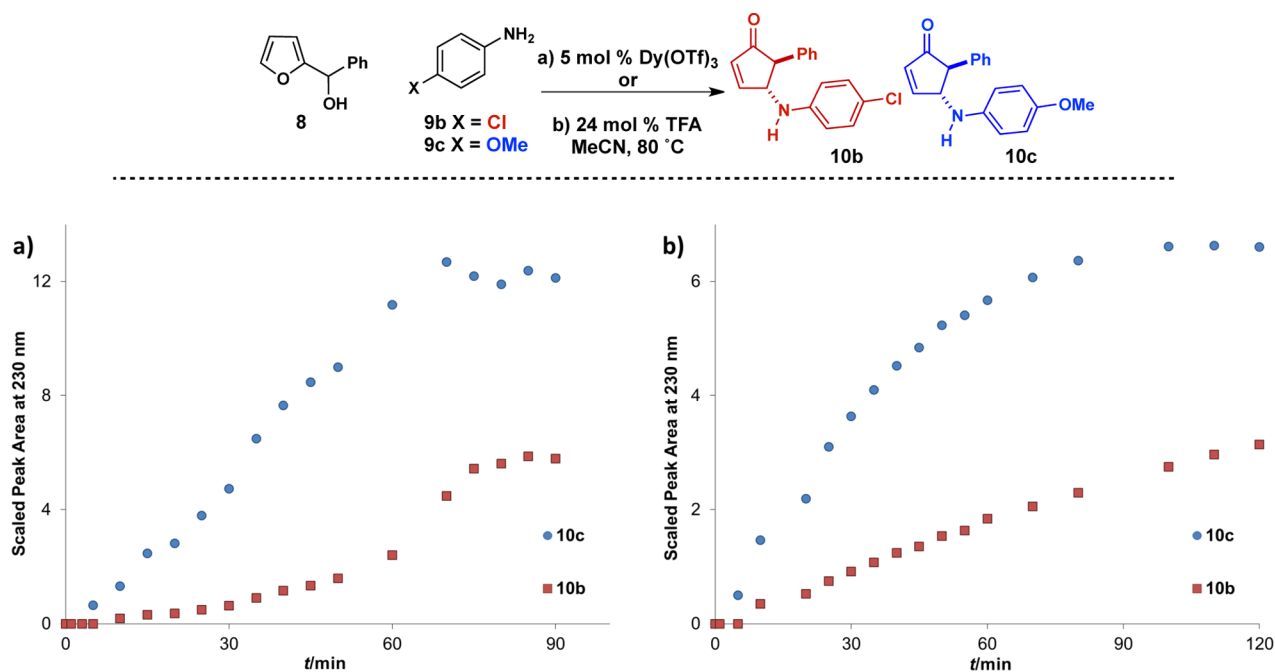
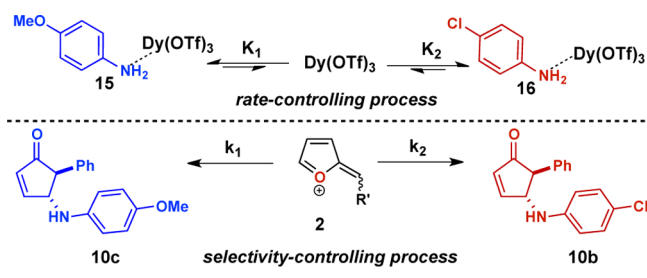


Figure 4. Competition between aniline nucleophiles: (a) $\text{Dy}(\text{OTf})_3$ -catalyzed system; (b) TFA-catalyzed system. Graphs showing UV peak area at 230 nm from HPLC/MS relative to 2-methoxynaphthalene as internal standard and scaled according to the relative extinction.

Scheme 3. Competitive Binding of $\text{Dy}(\text{OTf})_3$.



trifluoromethanesulfonate ($\text{Dy}(\text{OTf})_3$) was used as received from Strem Chemicals, Inc. All other materials were obtained from conventional suppliers and used as received. Flash chromatography was carried out using Sorbtech silica gel 60A (230 \times 400 mesh). Thin-layer chromatography (TLC) was performed on precoated silica gel plates and was visualized by irradiation with UV light or staining with potassium permanganate solution.

Kinetic studies monitored by in situ FTIR were conducted with a ReactIR iC 10 fitted with a Diamond ATR probe. Reaction temperatures were controlled using an internal temperature probe. 2-Methoxynaphthalene was used as an internal standard in some experiments as specified, and had no effect on the reaction, as confirmed by monitoring reactions via ReactIR and HPLC-MS both with and in the absence of the standard.

^1H NMR spectra (400, 500, or 600 MHz) and ^{13}C NMR spectra (125 MHz) are reported relative to residual proton signal from deuterated solvent. Data for ^1H NMR spectra are reported as follows: chemical shift (δ ppm), multiplicity, coupling constant (Hz) and integration. Data for ^{13}C NMR spectra are reported as follows: shift (δ ppm), multiplicity and coupling constant (Hz). IR spectra were recorded on a FT-IR spectrometer and are reported in terms of frequency of absorption (cm^{-1}). Mass spectra were obtained on a Micromass QTOF2 Quadrupole/TOF and GCT-Premier high resolution TOF equipped with an electrospray ionization source.

Validation of FTIR for Reaction Analysis.¹⁶ Validation of FTIR as a suitable technique for in situ reaction analysis was performed through reaction sampling and HPLC-MS analysis of reaction conversion and product formation as a function of time. The reaction

was sampled by withdrawal of approximately 5 μL aliquots of the reaction solution and diluted with methanol at room temperature. Samples were analyzed by HPLC-MS immediately. HPLC-MS analysis was conducted with an Agilent Eclipse XDB C18, 3.5 μm , 3.0 \times 75 mm column (standard column conditions: A = water (0.05% TFA), B = acetonitrile (0.05% TFA), 0.400 mL/min, initial, 38% B: linear gradient to 100% B over 20 min).

General Procedure for Kinetic Experiments. To a 10 mL vial with PTFE-silicon septum and open screw-cap was added 2 mL of acetonitrile. The vial was placed in a preheated oil bath at 80 $^\circ\text{C}$ and allowed to equilibrate. After taking a background scan in hot solvent, furan-2-yl(phenyl)methanol **8** (44.0 mg, 0.250 mmol, 0.125 M) and aniline **9a** (23.0 mg, 0.250 mmol, 0.125 M) were added to the pre-equilibrated acetonitrile. After a stable FTIR signal was observed, $\text{Dy}(\text{OTf})_3$ (7.6 mg, 0.013 mmol, 5 mol %) catalyst was added. Reaction progress was monitored by FTIR using two peaks: 1013 cm^{-1} for the consumption of furylcarbinol **8**, and 1715 cm^{-1} for the appearance of cyclopentenone **10a**.

Order in Trifluoroacetic Acid Catalyst.¹⁶ Stock solutions of **8**, **9a**, and trifluoroacetic acid (TFA) in acetonitrile were prepared and used within 2 days. Reactions were 0.125 M in **8** and **9a** and were run at 65 $^\circ\text{C}$. Concentrations of TFA were as follows: 3.125, 6.25, 12.5, 18.75, 25, and 30 mM. To a preheated vial of acetonitrile, the stock solutions of furylcarbinol **8** and aniline **9a** were added. When a steady signal was reached on the FTIR, an appropriate portion of the TFA stock solution was injected. The slope of the initial rate of formation of **9a** in each reaction was used in finding the order in TFA.

Order in $\text{Dy}(\text{OTf})_3$ Catalyst.¹⁶ Stock solutions of **8** and **9a** in acetonitrile were prepared and used within 2 days. Reactions were 0.125 M in **8** and **9a** and were run at 65 $^\circ\text{C}$. Concentrations of $\text{Dy}(\text{OTf})_3$ were as follows: 2, 4, 6.25, 8, 10, and 12 mM. To a preheated vial of acetonitrile were added the stock solutions of furylcarbinol **8** and aniline **9a**. When a steady signal was reached on the FTIR, the appropriate amount of $\text{Dy}(\text{OTf})_3$ was added as a solid. The slope of the initial rate of formation of **9a** in each reaction was used in finding the order in $\text{Dy}(\text{OTf})_3$.

Order in Furylcarbinol **8, TFA Catalyzed.**¹⁶ Stock solutions of **8** and **9a** in acetonitrile were prepared and used within 2 days. Reactions were 0.125 M in **8** and **9a** and were run at 65 $^\circ\text{C}$ on a 2 mL scale. To a preheated vial of acetonitrile, the stock solutions of furylcarbinol **8** and aniline **9a** were added. When a steady signal was reached on the FTIR,

0.02 mL of a 0.3 M TFA stock solution was used to provide a 2 mL reaction solution that was 30 mM in TFA (24 mol % relative to aniline 9a). The slope of the initial rate of formation of 10a in each reaction was used in finding order in furylcarbinol.

General Procedure for Linear Free Energy Relationship Analysis. A stock solution of 8 in acetonitrile was prepared and used within 2 days. Reactions were 0.125 M in 8 and the substituted aniline 9a–g and were run at 80 °C on a 2 mL scale. To a preheated vial of acetonitrile, the stock solutions of furylcarbinol 8 and the substituted aniline 9a–g were added. When a steady signal was reached on the FTIR, Dy(OTf)₃ (7.6 mg, 0.013 mmol, 5 mol % relative to furylcarbinol) was added as a solid. For the TFA-catalyzed experiments, 0.02 mL of a 0.3 M TFA stock solution was used to provide a 2 mL reaction solution that was 30 mM in TFA (24 mol % relative to furylcarbinol 8). The slopes of initial rate of formation of 10a–g in individual reactions were used in graphing the linear free energy relationship.

Nucleophile Competition Experiments. Competition experiments were conducted at 80 °C with 4-chloroaniline 9b and 4-methoxyaniline 9c to make cyclopentenones 10b and 10c, respectively. As a standard, 0.1 mL of a 0.101 M stock solution of 2-methoxynaphthalene for every 1 mL reaction solution was used. A 3 mL solution of acetonitrile and 2-methoxynaphthalene was preheated to 80 °C. Furylcarbinol 8 was added by dissolution from a tared syringe, followed by solid aniline 9b or 9c. A sample was taken at this point for analysis of initial conditions. Either Dy(OTf)₃ (5 mol % relative to furylcarbinol 8) or TFA (24 mol % relative to furylcarbinol 8) was added. The reactions were sampled by taking approximately 5 μL aliquots and dilution with approximately 1 mL of methanol and immediately analyzed by HPLC–MS.

General Procedure for Synthesis of Standard Products via Aza-Piancatelli Rearrangement. The furylcarbinol and aniline were dissolved in acetonitrile. To the reaction mixture at 23 °C was added 5 mol % of Dy(OTf)₃. The reaction flask was immediately fitted with a reflux condenser and placed in an oil bath preheated to 80 °C. Upon completion, as determined by TLC, the reaction was quenched with saturated aqueous sodium bicarbonate and extracted with ethyl acetate. The combined organic layers were dried over MgSO₄, filtered, and then concentrated in vacuo. The residue was purified by column chromatography to afford the desired cyclopentenone.

5-Phenyl-4-(phenylamino)cyclopent-2-enone (10a):¹⁷ ¹H NMR (500 MHz, CDCl₃) δ 7.76 (dd, *J* = 5.7, 2.3 Hz, 1H), 7.41–7.30 (m, 3H), 7.20–7.12 (m, 4H), 6.78 (dd, *J* = 10.6, 4.1 Hz, 1H), 6.57–6.51 (m, 2H), 6.41 (dd, *J* = 5.7, 1.6 Hz, 1H), 4.76 (bs, 1H), 4.11 (bs, 1H), 3.41 (d, *J* = 2.6 Hz, 1H) ppm; ¹³C NMR (125 MHz, CDCl₃) δ 206.7, 162.0, 146.3, 138.1, 134.7, 129.5, 129.1, 128.1, 127.5, 118.7, 113.9, 63.4, 60.1 ppm; IR (thin film) 3374, 3053, 3027, 1708, 1601, 1497, 1314 cm⁻¹; HRMS (ESI) *m/z* 272.1049 (272.1046 calcd for C₁₇H₁₅NNaO⁺ [M + Na]⁺).

4-((4-Chlorophenyl)amino)-5-phenylcyclopent-2-en-1-one (10b). According to the general procedure, Dy(OTf)₃ (4.4 mg, 0.0072 mmol, 0.05 equiv) was added to furan-2-yl(phenyl)methanol 8 (25.0 mg, 0.144 mmol, 1 equiv) and 4-chloroaniline 9b (18.3 mg, 0.144 mmol, 1 equiv) in 3 mL of acetonitrile. The resulting reaction mixture was heated to 80 °C for 10 min. The reaction was then quenched with 5 mL of saturated aqueous sodium bicarbonate and extracted with ethyl acetate (3 × 5 mL). The combined organic layers were dried over MgSO₄, filtered, and then concentrated in vacuo. The residue was purified by column chromatography to afford cyclopentenone 10b (41.2 mg, 90%) as a solid: ¹H NMR (600 MHz, CDCl₃) δ 7.74 (dd, *J* = 5.8, 2.3 Hz, 1H), 7.37–7.33 (m, 2H), 7.32–7.28 (m, 1H), 7.14–7.10 (m, 2H), 7.08–7.04 (m, 2H), 6.44–6.40 (m, 3H), 4.70 (q, *J* = 2.2 Hz, 1H), 4.13–4.02 (m, 1H), 3.36 (d, *J* = 2.6 Hz, 1H) ppm; ¹³C NMR (150 MHz, CDCl₃) δ 206.4, 161.4, 144.8, 138.0, 135.1, 129.4, 129.2, 128.0, 127.6, 123.4, 115.0, 63.5, 60.2 ppm; IR (thin film) 3375, 3060, 3029, 2924, 2854, 1870, 1803, 1702, 1597, 1492, 1314, 1248, 1178, 1090 cm⁻¹; HRMS (ESI) *m/z* 306.0655 (306.0662 calcd for C₁₇H₁₄ClNNaO⁺ [M + Na]⁺); MS (ESI) *m/z* 284.09 (100), 286.1 (34), 285.10 (20), 287.10 (6) (284.08, 286.08, 285.09, 287.08 calcd for C₁₇H₁₅ClNO⁺ [M + H]⁺).

4-((4-Methoxyphenyl)amino)-5-phenylcyclopent-2-enone (10c):¹⁷ ¹H NMR (500 MHz, CDCl₃) δ 7.78 (dd, *J* = 5.7, 2.3 Hz, 1H), 7.38–7.24 (m, 3H), 7.12 (d, *J* = 7.2 Hz, 2H), 6.72 (d, *J* = 8.9 Hz, 2H), 6.51 (d, *J* = 8.9 Hz, 2H), 6.39 (dd, *J* = 5.7, 1.5 Hz, 1H), 4.67 (d, *J* = 1.7 Hz, 1H), 3.73 (s, 3H), 3.38 (d, *J* = 2.5 Hz, 1H) ppm; ¹³C NMR (125 MHz, CDCl₃) δ 206.9, 162.3, 153.2, 140.2, 138.3, 134.8, 129.1, 128.2, 127.5, 115.8, 115.1, 64.6, 60.1, 55.8 ppm; IR (thin film) 3363, 3031, 2935, 2835, 1709, 1593, 1512, 1242 cm⁻¹; HRMS (ESI) *m/z* 302.1154 (302.1151 calcd for C₁₈H₁₇NNaO₂⁺ [M + Na]⁺).

4-((4-Iodophenyl)amino)-5-phenylcyclopent-2-enone (10d):¹⁷ ¹H NMR (500 MHz, CDCl₃) δ 7.72 (dd, *J* = 5.7, 2.4 Hz, 1H), 7.40–7.28 (m, 5H), 7.15–7.09 (m, 2H), 6.40 (dd, *J* = 5.7, 1.7 Hz, 1H), 6.27 (dddd, *J* = 9.8, 2.0, 2.0, 2.0 Hz, 2H), 4.69 (dd, *J* = 8.2, 1.7 Hz, 1H), 4.19 (d, *J* = 8.3 Hz, 1H), 3.35 (d, *J* = 2.6 Hz, 1H) ppm; ¹³C NMR (125 MHz, CDCl₃) δ 206.4, 161.5, 145.9, 138.0, 137.9, 135.0, 129.2, 128.0, 127.6, 116.0, 79.6, 63.2, 60.1 ppm; IR (thin film) 3776, 3026, 1704, 1588, 1496, 1316 cm⁻¹; HRMS (ESI) *m/z* 398.0022 (398.0012 calcd for C₁₇H₁₄INNaO⁺ [M + Na]⁺).

4-((4-Bromophenyl)amino)-5-phenylcyclopent-2-en-1-one (10e). According to the general procedure, Dy(OTf)₃ (4.4 mg, 0.0072 mmol, 0.05 equiv) was added to furan-2-yl(phenyl)methanol 8 (25.0 mg, 0.144 mmol, 1 equiv) and 4-bromoaniline 9e (24.7 mg, 0.144 mmol, 1 equiv) in 3 mL of acetonitrile. The resulting reaction mixture was heated to 80 °C for 15 min. The reaction was then quenched with 5 mL of saturated aqueous sodium bicarbonate and extracted with ethyl acetate (3 × 5 mL). The combined organic layers were dried over MgSO₄, filtered, and then concentrated in vacuo. The residue was purified by column chromatography to afford 10e (36.4 mg, 76%) as a solid: ¹H NMR (600 MHz, CDCl₃) δ 7.75 (dd, *J* = 5.8, 2.4 Hz, 1H), 7.38–7.32 (m, 2H), 7.33–7.27 (m, 1H), 7.23–7.17 (m, 2H), 7.16–7.10 (m, 2H), 6.44 (dd, *J* = 5.8, 1.7 Hz, 1H), 6.40–6.36 (m, 2H), 4.73–4.70 (m, 1H), 4.00 (d, *J* = 8.5 Hz, 1H), 3.36 (d, *J* = 2.6 Hz, 1H) ppm; ¹³C NMR (150 MHz, CDCl₃) δ 206.3, 161.2, 145.2, 138.0, 135.2, 132.3, 129.2, 128.0, 127.7, 115.5, 110.6, 63.5, 60.2 ppm; IR (thin film) 3369, 3061, 3027, 2920, 1700, 1591, 1487, 1313 cm⁻¹; HRMS (ESI) *m/z* 350.0145 (350.0156 calcd for C₁₇H₁₄BrNNaO⁺ [M + Na]⁺); MS (ESI) *m/z* 352.02 (100), 350.02 (96), 351.02 (18), 353.02 (15) (352.01, 350.02, 351.02, 353.02 calcd for C₁₇H₁₄BrNNaO⁺ [M + Na]⁺).

4-((4-Fluorophenyl)amino)-5-phenylcyclopent-2-en-1-one (10f). According to the general procedure, Dy(OTf)₃ (8.7 mg, 0.014 mmol, 0.05 equiv) was added to furan-2-yl(phenyl)methanol 8 (50.0 mg, 0.287 mmol, 1 equiv) and 4-fluoroaniline 9f (27.0 μL, 0.287 mmol, 1 equiv) in 3 mL of acetonitrile. The resulting reaction mixture was heated to 80 °C for 2.5 h. The reaction was then quenched with 5 mL of saturated aqueous sodium bicarbonate and extracted with ethyl acetate (3 × 5 mL). The combined organic layers were dried over MgSO₄, filtered, and then concentrated in vacuo. The residue was purified by column chromatography to afford cyclopentenone 10f (70.5 mg, 92%) as a solid: ¹H NMR (500 MHz, CDCl₃) δ 7.77 (dd, *J* = 5.7, 2.3 Hz, 1H), 7.38–7.27 (m, 3H), 7.15–7.08 (m, 2H), 6.88–6.80 (m, 2H), 6.48–6.44 (m, 2H), 6.42 (dd, *J* = 5.8, 1.7 Hz, 1H), 4.69 (s, 1H), 3.87 (s, 1H), 3.37 (d, *J* = 2.6 Hz, 1H) ppm; ¹³C NMR (150 MHz, CDCl₃) δ 206.5, 161.7, 156.6 (d, *J* = 237.0 Hz), 142.5, 138.1, 135.0, 129.2, 128.0, 127.57, 116.0 (d, *J* = 22.5 Hz), 115.2 (d, *J* = 7.5 Hz), 64.2, 60.2; IR (thin film) 3370, 3061, 3029, 2918, 1701, 1505, 1309, 1213, 1156 cm⁻¹; HRMS (ESI) *m/z* 267.1053 (267.1059 calcd for C₁₇H₁₄FNO⁺ [M]⁺).

Methyl 4-((4-oxo-5-phenylcyclopent-2-en-1-yl)amino)benzoate (10g):¹⁷ ¹H NMR (500 MHz, CDCl₃) δ 7.83–7.77 (m, 2H), 7.75 (dd, *J* = 5.7, 2.3 Hz, 1H), 7.41–7.29 (m, 3H), 7.16–7.10 (m, 2H), 6.49–6.42 (m, 3H), 4.82 (dddd, *J* = 8.1, 2.2, 2.2, 2.2 Hz, 1H), 4.63 (d, *J* = 8.3 Hz, 1H), 3.84 (s, 3H), 3.39 (d, *J* = 2.6 Hz, 1H) ppm; ¹³C NMR (125 MHz, CDCl₃) δ 206.2, 167.2, 161.0, 150.3, 137.8, 135.3, 131.7, 129.3, 128.1, 127.8, 119.8, 112.6, 62.8, 60.3, 51.8 ppm; IR (thin film) 3359, 3023, 2950, 1705, 1604, 1280 cm⁻¹; HRMS (ESI) *m/z* 330.1106 (330.1101 calcd for C₁₉H₁₇NNaO₃⁺ [M + Na]⁺).

■ ASSOCIATED CONTENT

📄 Supporting Information

^1H and ^{13}C NMR spectra and calibration data for kinetic measurements. This material is available free of charge via the Internet at <http://pubs.acs.org>.

■ AUTHOR INFORMATION

Corresponding Author

*E-mail: jhein2@ucmerced.edu.

Notes

The authors declare no competing financial interest.

■ ACKNOWLEDGMENTS

Funding from UCM (GRC Faculty Research Award), UCSB, and the National Science Foundation (CAREER Award CHE-1057180-JR) is gratefully acknowledged. Additional support provided by the UCSB Graduate Research Mentorship Program Fellowship (G.K.V.), UCM-Graduate Division Fellowship (D.Y.), and Mettler-Toledo AutoChem.

■ REFERENCES

- (1) (a) Piancatelli, G.; Scettri, A.; Barbadoro, S. *Tetrahedron Lett.* **1976**, *17*, 3555–3558. (b) For a review, see: Piancatelli, G.; D'Auria, M.; D'Onofrio, F. *Synthesis* **1994**, 867–889.
- (2) (a) Veits, G. K.; Wenz, D. R.; Read de Alaniz, J. *Angew. Chem., Int. Ed.* **2010**, *49*, 9484–9487. (b) Palmer, L. I.; Read de Alaniz, J. *Angew. Chem., Int. Ed.* **2011**, *50*, 7167–7170.
- (3) Palmer, L. I.; Read de Alaniz, J. *Org. Lett.* **2013**, *15*, 476–479.
- (4) (a) Yin, B.-L.; Lai, J.-Q.; Zhang, Z.-R.; Jiang, H.-F. *Adv. Synth. Catal.* **2011**, *353*, 1961–1965. (b) Yin, B.; Huang, L.; Zhang, X.; Ji, F.; Jiang, H. *J. Org. Chem.* **2012**, *77*, 6365–6370. (c) Yin, B.; Huang, L.; Wang, X.; Liu, J.; Jiang, H. *Adv. Synth. Catal.* **2013**, *355*, 370–376.
- (5) (a) Faza, O. N.; López, C. S.; Álvarez, R.; de Lera, Á. R. *Chem.—Eur. J.* **2004**, *10*, 4324–4333. For a related review, see: (b) Davis, R. L.; Tantillo, D. J. *Curr. Org. Chem.* **2010**, *14*, 1561–1577.
- (6) Rosenfeld, D. C.; Shekhar, S.; Takemiya, A.; Utsunomiya, M.; Hartwig, J. F. *Org. Lett.* **2006**, *8*, 4179–4182 and references therein.
- (7) Triflic acid does catalyze the reaction; however, we observed byproducts arising from product rearrangement and Friedel–Crafts alkylation.
- (8) See the Supporting Information for plots of rate dependence on both TFA and $\text{Dy}(\text{OTf})_3$ concentration.
- (9) (a) Gao, Y.; Wu, W.-L.; Ye, B.; Zhou, R.; Wu, Y.-L. *Tetrahedron Lett.* **1996**, *37*, 893–896. (b) Yin, B.-L.; Yang, Z.-M.; Hu, T.-S.; Wu, Y.-L. *Synthesis* **2003**, 1995–2000. (c) Chen, L.; Xu, H.-H.; Yin, B.-L.; Xiao, C.; Hu, T.-S.; Wu, Y.-L. *J. Agric. Food. Chem.* **2004**, *52*, 6719–6723.
- (10) Berg, J.; Tymoczko, J.; Stryer, L. *Biochemistry*; W. H. Freeman and Co.: New York, 2002; ISBN 0-7167-4955-6.
- (11) See the Supporting Information for our full derivation of this equation
- (12) (a) Burin, M. E.; Fukin, G. K.; Bochkarev, M. N. *Russ. Chem. Bull.* **2007**, *56*, 1736–1741. (b) Rzączyńska, Z.; Woźniak, M.; Wołodkiewicz, W.; Ostasz, A.; Pikus, S. *J. Therm. Anal. Calorim.* **2007**, *88*, 871–876.
- (13) Hein, J. E.; Armstrong, A.; Blackmond, D. G. *Org. Lett.* **2011**, *13*, 4300–4303.
- (14) LCMS analysis of reactions A and B show byproducts consistent with Friedel–Crafts reaction; see ref 2a.
- (15) Csáký, A. G.; Mba, M.; Plumet, J. *Synlett* **2003**, *13*, 2092–2094.
- (16) See the Supporting Information for more detail.
- (17) Characterization from the original report; see ref 2a.